

# Linear-least-squares-fitting procedure for the solution of a time-dependent wave function of a model atom in a strong laser field in the Kramers-Henneberger frame

Xiaoxin Zhou,<sup>1,2</sup> Baiwen Li,<sup>1,3</sup> and C. D. Lin<sup>4</sup>

<sup>1</sup>*Wuhan Institute of Physics and Mathematics, The Chinese Academy of Science, Wuhan 430071, People's Republic of China*

<sup>2</sup>*Department of Physics, Northwest Normal University, Lanzhou, Gansu 730070, People's Republic of China*

<sup>3</sup>*Chinese Center of Advanced Science and Technology (World Laboratory), P.O. Box 8370, Beijing, People's Republic of China*

<sup>4</sup>*Department of Physics, Kansas State University, Manhattan, Kansas 66506-2601*

(Received 2 April 2001; published 12 September 2001)

We present a linear-least-squares-fitting method to solve the time-dependent Schrödinger equation of a one-dimensional model atom in an intense laser field in the Kramers-Henneberger frame. In comparison with calculations in the laboratory frame, it is shown that in the Kramers-Henneberger frame, the method is more stable and larger time steps in the propagation can be used. The fitting procedure also allows for easy change of basis functions during the time propagation. The method is applied to study the stabilization of a model atom in an intense laser field where the electron is bound initially by a one-dimensional soft Coulomb potential.

DOI: 10.1103/PhysRevA.64.043403

PACS number(s): 42.50.Hz, 32.80.Qk, 32.80.Rm, 32.80.Wr

## I. INTRODUCTION

In the past decades, direct numerical integration of the time-dependent Schrödinger equation (TDSE) has been employed to interpret many experimental findings for atoms in an intense laser field [1–5]. In a previous paper [6], we have proposed an approach for solving the TDSE by expanding the time-dependent wave functions in terms of field-free eigenstates, where the expansion coefficients are solved using a linear-least-squares-fitting technique [7]. The linear-least-squares-fitting procedure allows us to avoid the evaluation of many matrix elements, as occurred in the standard close-coupling or eigenfunction expansion method. The numerical results for harmonic generation were in good agreement with those calculated with the split-operator method. Unlike the split-operator method and other methods, the least-squares method does not require the introduction of absorber at boundaries. The fitting procedure automatically filters out high-frequency oscillations near the boundary that may result from the interference between the outgoing wave and the reflected wave. However, the calculated probability distribution from the two methods do not agree satisfactorily at large distances, or near the boundaries, after propagating for a long time. It appears that the linear-least-squares-fitting procedure, while removing the unphysical interference from the boundaries, also removed some fast oscillation amplitudes in the wave functions. When the time step was reduced (for instance,  $\Delta t \leq 0.01$  a.u.), the probability distributions would agree with those obtained by the split-operator method if the absorber were implemented at the boundaries for each method. However, the introduction of the absorber on the boundaries increases the computation time significantly, especially for laser pulses with long duration or of many cycles. In order to solve the TDSE using basis set expansion, it is desirable that the wave function does not oscillate rapidly such that the time-dependent expansion coefficients can be integrated without resorting to very small time steps. In [6], the time-dependent wave function was integrated in the laboratory frame. It is well known that the

time-dependent wave function of an electron in a laser field is better represented in the so-called Kramers-Henneberger (KH) frame [8–10]. In this frame, the free electron is at rest, while the nucleus quivers with the laser frequency. In the KH frame, the electronic wave function does not depend strongly on time and it is expected that calculations of the wave function in the KH frame using the linear-least-squares method would be more efficient and stable such that the calculation can be carried out over a longer time period and/or at a higher-laser field intensity. The increased numerical prowess would allow us to study the issue of stabilization of atoms in a laser field at sufficiently high intensities [11–13].

In the KH frame, a free electron in the laser field is at rest, the sum of the Coulomb potential and the time-dependent laser-atom interaction in the laboratory frame is replaced by a time-dependent KH potential. The main advantage of the KH frame is that it is very suitable for studying the stabilization of atoms at sufficiently high intensities and frequencies because the effective time-dependent potential is replaced approximately by a time-averaged static potential, with the higher-order time dependence taken as a small perturbation. In recent years, a number of theoretical studies on the ionization of atoms in laser fields have been carried out by using the finite-difference method [10,12–15], the finite-elements method [16], the split-operator method [17–19], the close-coupling method [20–23], the Floquet theory [24–28], and the classical method [29]. So far, to our knowledge, there are few studies on the interaction of atoms with very strong laser fields in the KH frame using the close-coupling method. The reason is because the matrix elements of the KH potential are time dependent and the calculation of matrix elements in each time step is very time consuming. As mentioned above, the linear-least-squares-fitting method avoids the calculation of matrix elements and the method can be easily implemented to integrate the TDSE in the KH frame. As we will see later, there are additional advantages in propagating the TDSE in the KH frame. In Sec. II, the theoretical method will be briefly outlined. The numerical results are presented in Sec. III to show the advantage of calculating the wave functions in the KH frame and the study of

stabilization in an intense laser field. A short summary is given in Sec. IV.

## II. THEORETICAL METHOD

We consider a one-dimensional model atom in a laser field. Within the dipole approximation, the time-dependent Schrödinger equation in the velocity gauge is given by (atomic units are used throughout this paper)

$$i\frac{\partial\psi(x,t)}{\partial t} = \left[ \frac{1}{2} \left( p + \frac{1}{c} A(t) \right)^2 + V(x) \right] \psi(x,t) \quad (1)$$

in the laboratory frame where  $V(x)$  is taken to be the soft Coulomb potential [15,30,31]

$$V(x) = -\frac{1}{\sqrt{1+x^2}}. \quad (2)$$

In Eq. (1)  $A(t)$  is the vector potential of the driving laser field and  $E(t) = -(1/c)dA(t)/dt$  is the electric field. Following Kramers [8] and Henneberger [9], a unitary transformation (see also [10])

$$U = \exp(-i\hat{T}), \quad (3)$$

with

$$\hat{T} = -\frac{1}{c} \int_0^t A(\tau) d\tau p + \frac{1}{2c^2} \int_0^t A^2(\tau) d\tau, \quad (4)$$

gives the time-dependent Schrödinger equation in the KH frame

$$i\frac{\partial}{\partial t} \psi_{KH}(x,t) = H_{KH}(x,t) \psi_{KH}(x,t), \quad (5)$$

where  $H_{KH}(x,t) = (1/2)p^2 + V[x - \alpha(t)]$ , and  $\psi_{KH}(x,t) = U\psi(x,t)$  are the Hamiltonian and the wave function in the KH frame, respectively, with  $\alpha(t) = -(1/c) \int_0^t A(\tau) d\tau$  being the classical displacement of a free electron in the laser field, and  $V[x - \alpha(t)]$  is called the KH potential. Thus, in the KH frame the electron-laser interaction is removed but the electron-nucleus potential,  $V(x)$  is replaced by a time-dependent potential  $V[x - \alpha(t)]$  where the position of the electron is shifted by a time-dependent displacement  $\alpha(t)$ . For convenience, here we write the TDSE in length gauge as the following:

$$i\frac{\partial\varphi(x,t)}{\partial t} = \left( -\frac{1}{2}p^2 + V(x) - xE(t) \right) \varphi(x,t), \quad (6)$$

where the  $\psi(x,t)$  of Eq. (1) in the velocity gauge and  $\varphi(x,t)$  in the length gauge are connected by the relation

$$\psi(x,t) = \exp\left(\frac{i}{c}xA(t)\right) \varphi(x,t). \quad (7)$$

By comparing Eqs. (5) and (6), it is clear that the interaction potential does not increase with  $x$  in the KH frame, which makes the numerical calculation more stable and tractable.

In our calculations, we chose a laser field profile

$$E(t) = \begin{cases} E_0 \sin^2\left(\frac{\pi t}{6T}\right) \sin \omega t, & 0 \leq t \leq 3T \\ E_0 \sin \omega t, & t > 3T, \end{cases} \quad (8)$$

where  $E_0$  is the amplitude, and  $T$  the period of the laser field. Thus, the field is turned on to the maximum amplitude over  $3T$ .

We solved the time-dependent Schrödinger equation (5) using a linear-least-squares fitting technique as described in [6]. In this approach, the time-dependent wave function is first expanded as

$$\psi_{KH}(x,t) = \sum_{n=1}^N c_n(t) \phi_n(x), \quad (9)$$

where the basis functions  $\phi_n(x)$  are constructed from the  $B$ -spline functions and the sine and cosine functions. The  $B$  splines are used to construct the bound states mostly, while the sine and cosine functions are used to generate pseudostates to represent the continuum spectrum. Within the basis set selected, the solution of Eq. (5) is reduced to a set of linear first-order differential equations

$$i \sum_{n=1}^N \frac{dc_n(t)}{dt} \phi_n(x,t) = \sum_{n=1}^N H_{KH}(x,t) c_n(t) \phi_n(x). \quad (10)$$

In the conventional approach one would project this equation into the space spanned by the basis set. For a set of  $N$  basis functions, this would require the evaluation of roughly  $N^2$  matrix elements, many of them involving oscillatory functions. An alternative method proposed by Sidky and Lin [7] was adopted by us in [6] to solve the time-dependent Schrödinger equation (6). In this method, the spatial coordinate  $x$  is discretized into  $M$  points where  $M$  is greater than  $N$ . By evaluating Eq. (10) at the discretized points, the resulting equations are then solved by the linear-least-squares-fitting method. The details of the method is given in [6]. In the present paper, we applied this method in solving the time-dependent Schrödinger equation (5) in the KH frame.

Before presenting the numerical results, it is important to point out the advantage of performing the calculations in the KH frame. To carry out Runge-Kutta integration forward at each time step, accurate values of  $dc_n(t)/dt$  must be obtained. For calculations in the length gauge [see Eq. (6)], the values of  $dc_n(t)/dt$  depend on both  $E(t)x \sin(m\pi x/x_{\max})$  [or  $\cos(m\pi x/x_{\max})$ ] and  $V(x)\sin(m\pi x/x_{\max})$  or  $\cos(m\pi x/x_{\max})$  where the sine and cosine functions are from the basis functions. When  $m$  is large, the contribution from the former term varies rapidly with  $x$  for large  $x$ . To achieve accurate numerical result, one would need very closed-space discretized points at large  $x$  and integrate with very small time steps. This is the problem encountered in [6] when the linear-least-

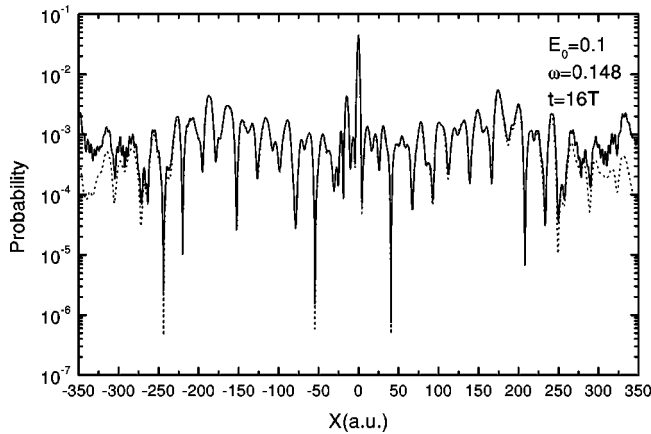


FIG. 1. Probability density of the time-dependent wave function at  $t=16$  T. The solid line is calculated in the KH frame ( $\Delta t=0.16$  a.u.), and the dotted line is calculated in the laboratory frame ( $\Delta t=0.02$  a.u.). Both results use the same parameters except the time steps.

squares method was applied to Eq. (6) in the laboratory frame. In the KH frame, on the other hand, the values of  $dc_n(t)/dt$  depend only on  $V[x-\alpha(t)]\sin(m\pi x/x_{\max})$  [or  $\cos(m\pi x/x_{\max})$ ]. Since the potential  $V(x)$  decreases smoothly at large  $x$ , the right-hand side of Eq. (5) would not become large at large  $x$ . Furthermore, the KH potential changes smoothly from time  $t$  to  $t+\Delta t$ , thus, it is possible to take a larger  $\Delta t$  in the time propagation.

### III. NUMERICAL RESULTS

To illustrate the method, we compare in Fig. 1 the probability density of the wave function at time  $t=16$  T for a laser with amplitude  $E_0=0.1$  a.u. and frequency  $\omega=0.148$  a.u. calculated in the laboratory frame and in the KH frame. We have employed equally spaced grid points with  $\Delta x=0.39$  and  $x_{\max}=400$  and a basis set of  $N=700$ . In both cases, identical absorber at the boundaries were used. From Fig. 1, the two results are essentially identical except at the outer region. However, to achieve the accuracy needed, a time step of  $\Delta t=0.02$  had to be used for calculations in the laboratory frame. In the KH frame, the same accuracy can be achieved by using  $\Delta t=0.16$ . The computation time was found to be about six times smaller. As a check, we even took  $\Delta t=0.32$  and reasonable results were still obtained. As a further check, we also obtained the above-threshold ionization (ATI) spectra by using the same parameters as in Fig. 1, but at time  $t=6.25$  T where little ionized electron wave packet has arrived at the boundaries yet. Clearly, the present two calculations, as shown in Fig. 2, give essentially identical ATI peaks.

The least-squares-fitting procedure not only avoids the evaluation of matrix elements, but also offers an easy way to change the basis functions during the time integration. It has the advantage of being able to switch to basis functions tailored to the problem at different regimes. In the following, we show how this method is implemented to investigate the stabilization of atoms in very high-intense fields, especially

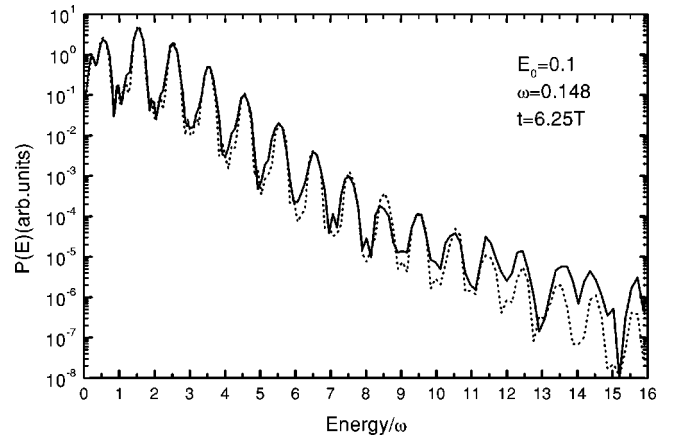


FIG. 2. ATI spectra at  $t=6.25$  T. The parameters used are the same as in Fig. 1. Symbols as in Fig. 1.

at high frequencies. This subject has been extensively investigated theoretically (for instance, [15,17,18], and references therein). Experimentally, the stabilization has been observed for Rydberg atoms [32]. In a realistic experiment, the high field has to be turned on over a certain finite time. It is possible that the atom is fully ionized before the high field is reached, and thus, stabilization would not occur. As pointed out previously [10,15,33], the wave function of the electron is better described by KH eigenstates that are eigenstates of the time-average KH potential

$$\left[ -\frac{1}{2} \frac{d^2}{dx^2} + V_0(\alpha_0, x) \right] \chi(\alpha_0, x) = E_{KH}^0 \chi(\alpha_0, x), \quad (11)$$

where  $\alpha_0 = E_0/\omega^2$  is the maximum classical displacement of the electron in the constant field, and

$$V_0(\alpha_0, x) = \frac{1}{T} \int_0^T V(x - \alpha_0 \sin \omega t) dt, \quad (12)$$

is the time-averaged part of the KH potential. However, this basis set is not easily implemented to describe the initial state since it is the eigenstate of the field-free atom. Thus, the procedure we adopted is to expand the time-dependent wave function in terms of basis functions of the field-free atom during the laser turn-on period. After the turn on, KH eigenstates are used as basis functions. With the fitting procedure, the change of basis functions requires little modification of the code. Using the  $B$  splines and the sine and cosine functions as primitive functions, the KH eigenstates are easily obtained by solving the above equation (11) in the basis spanned. Note that the KH eigenstates depend only on  $\alpha_0$ .

As a test of this method, we propagate Eq. (5) using the field-free eigenstates as basis functions at the turn-on stage and the KH eigenstates once the field is fully on. The least-squares-fitting method was used to solve the time-dependent equation. In Fig. 3 we show calculations carried out for three situations where  $\alpha_0=4$  a.u., with differing laser frequencies and field strengths. Shown are the population weights of the ground state, the first excited state, and the total bound states, all are referred with respect to the KH eigenstates.

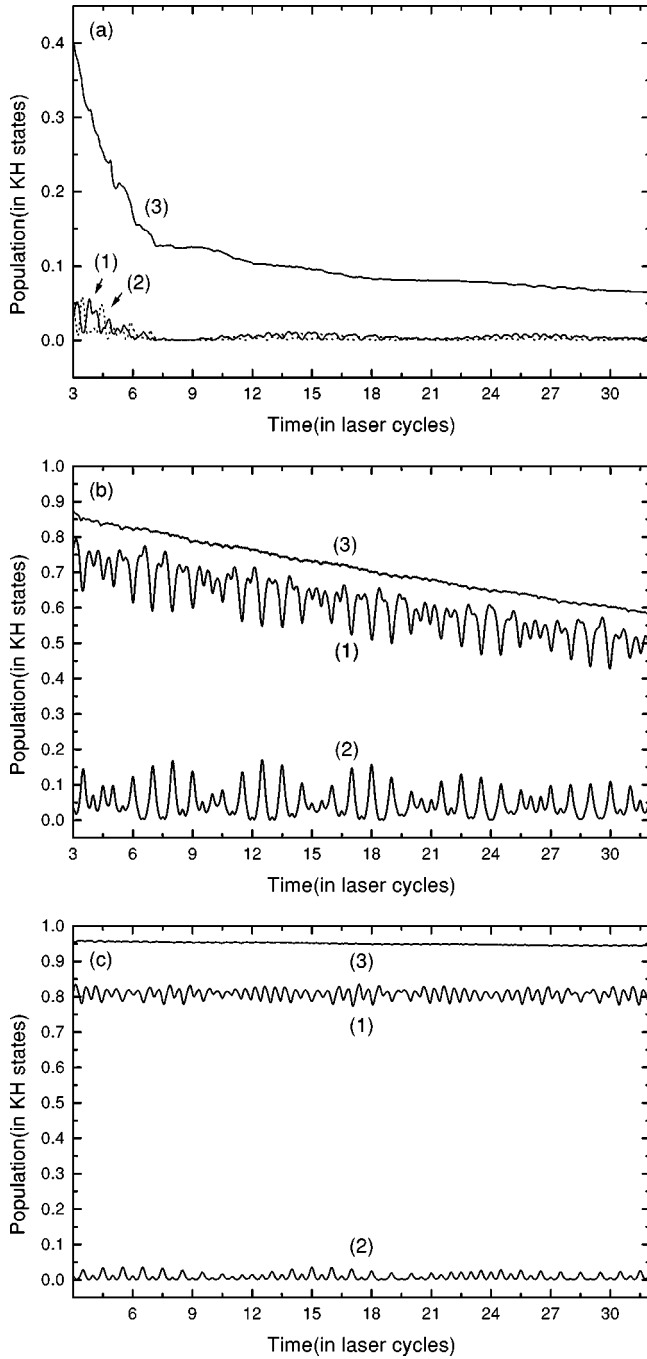


FIG. 3. Population distributions of the KH states, (1) the ground state, (2) the first excited state, and (3) total bound states, as a function of time after the laser pulse turn on. (a)  $E_0=0.36$ ,  $\omega=0.3$ ; (b)  $E_0=4$ ,  $\omega=1$ ; (c)  $E_0=16$ ,  $\omega=2$ .

In Fig. 3, the population of the ground state, the first excited state, and total bound states of the KH time-average potential are plotted as a function of time for different intensities and frequencies. Because the population of the KH states has no meaning during the turn-on time period, we only show results after the laser is fully turned on. The laser pulse used is the same as given in Eq. (8), and the parameters used are  $x_{\max}=300$ ,  $N=650$ ,  $\Delta x=0.3$ ,  $\Delta t=0.1$  to  $0.2$ . At the modest strong field,  $E_0=0.36$ , and frequency  $\omega=0.3$

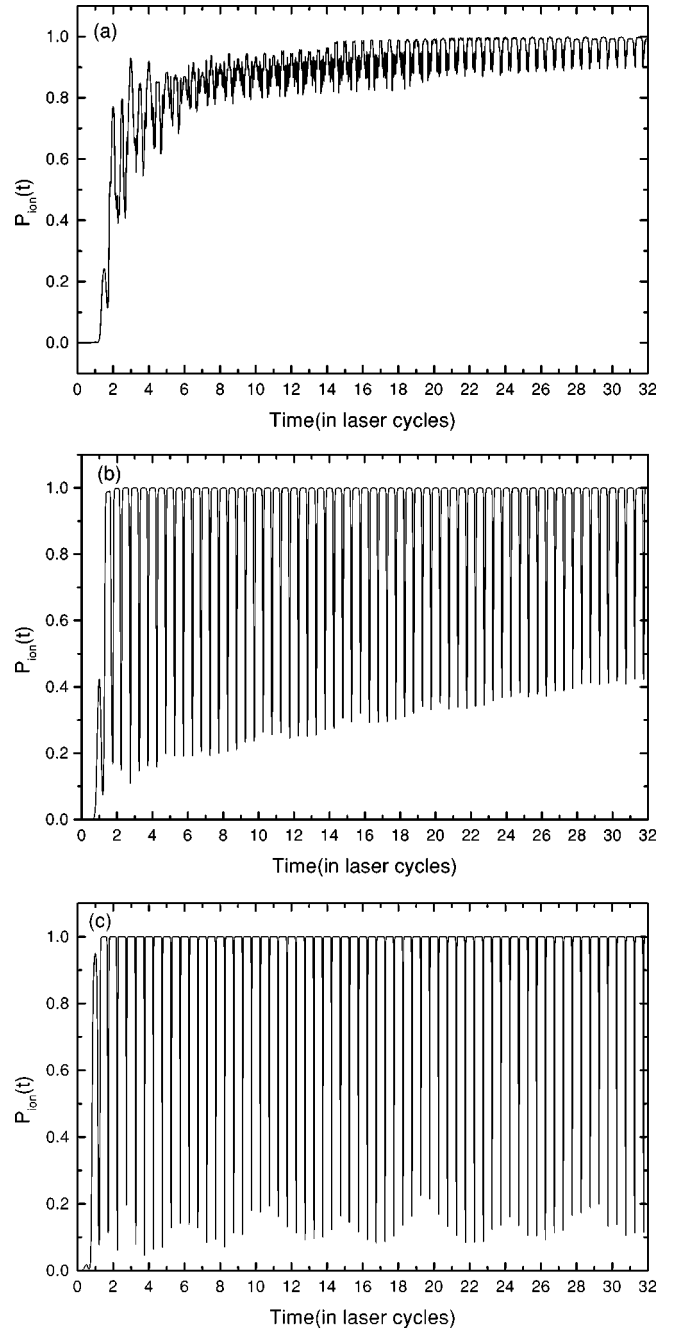


FIG. 4. Ionization probability as a function of time in the laboratory frame, using the same parameters as in Fig. 3, respectively.

[see Fig. 3(a)], the total population in the KH bound states decreases rapidly with time, then stabilizes at 0.07, while the populations in the KH ground state and the first excited state are negligible after six cycles. However, for  $\omega=1$ , and  $E_0=4$ , as shown in Fig. 3(b), the populations of the KH ground and first excited states account for almost the total bound population, and the two populations oscillate with time and decrease linearly. These results are similar to those of Ref. [10] where calculations were carried out in the KH frame for a short-range potential chosen to have only two bound states. Their method required calculations of the overlap of KH eigenstates.

The oscillations in the individual bound-state populations can be interpreted as due to the “residual” time-dependent part of the KH potential that would affect the time-dependent wave function if  $\omega$  is not very high [In Fig. 3(a), the oscillation is less clear since the amplitudes for the ground and the first excited states are small]. Furthermore, the total population in the KH bound states does not oscillate much and decreases linearly with time slowly. This indicates that the atomic system is stabilizing and there is little ionization with increasing time. For the higher laser frequency  $\omega=2$  and field strength  $E_0=16$  [see Fig. 3(c)], the total KH bound-state population remains constant, the populations of the KH ground and first excited states also remain nearly constant with the atom mostly in the ground state. The small oscillation in the bound-state population is due to the residual time-dependent part of the KH potential. In this case, the atom is nearly completely stabilized right after the turn-on step.

In order to obtain the ionization probability with time in the laboratory frame, we need to transform  $\varphi_{KH}(x,t)$  back to the laboratory frame via the unitary transformation Eqs. (3) and (4), and Eq. (14) in Ref. [6]. The time-dependent ionization probabilities  $P_{ion}(t)$  for the three sets of parameters of Fig. 3 are shown in Fig. 4. In case (a), 90% has been ionized on the average at the end of 32 laser cycles, while in the stabilization region [in the case of (b) and (c)], the ionization probability  $P_{ion}(t)$  changes rapidly between one and a minimum within each cycle, this minimum decreases with increasing field strength. The figures also show that in the stabilization region, the electron changes rapidly between the bound states and the continuum states (of the field-free Hamiltonian) in the laboratory frame, unlike in the KH frame, where stabilization is reflected by a stable large population of the ground-state wave function in the KH frame. This suggests that it is better to describe stabilization in terms of the population distributions in the KH frame. When

stabilization occurs, the wave function in the KH frame does not change significantly within each cycle. The rapid variation of ionization probability over a laser cycle in Fig. 4(b) and 4(c) is due to the quiver energy of the electron. In an actual experiment, ionization is measured after the laser pulse has been turned off. Thus, it is expected that the ionization probability in the stabilization regime will depend sensitively on the turn off of the laser pulse.

#### IV. SUMMARY

In summary, we showed the application of the linear-least-squares-fitting procedure in solving the time-dependent Schrödinger equation for atoms in an intense laser field in the KH frame. Comparing to the solution in the laboratory frame, we showed that calculations can be carried out in the KH frame with a much larger time step to reduce the computational demand. The fitting procedure also allows easy change of basis functions. Combining with the use of the KH frame, we have investigated the stabilization in an intense laser field using two sets of basis functions, one suitable for the laser turn-on region and the other using KH eigenstates. It should be noted that the stabilized cases (b) and (c) in Figs. 3 and 4 cannot be obtained using the fitting procedure in the laboratory frame even if time step of  $\Delta t=0.01$  is used. In the KH frame, calculations using time step of  $\Delta t=0.05$  to  $0.1$  can still give accurate results.

#### ACKNOWLEDGMENTS

This paper was supported in part by the National Science Foundation of China under Grant Nos. 19734060, and 19874051. C.D.L. acknowledges support in part by Chemical Sciences, Geosciences and Biosciences Division, Office of Basic Energy Sciences, Office of Science, and the U. S. Department of Energy.

- 
- [1] M. Protopapas, C.H. Keitel, and P.L. Knight, *Rep. Prog. Phys.* **60**, 389 (1997).
  - [2] M. Gavrilu, *Atoms in Intense Laser Fields*, edited by M. Gavrilu (Academic, New York, 1992), p. 435.
  - [3] K. Burnett, V.C. Reed, and P.L. Knight, *J. Phys. B* **26**, 561 (1993).
  - [4] C.J. Joachain, M. Dörr, and N.J. Kylstra, *Adv. At., Mol., Opt. Phys.* **42**, 225 (1999).
  - [5] P. Salières, A. L’Huillier, P. Antoine, and M. Lewenstein, *Adv. At., Mol., Opt. Phys.* **41**, 83 (1999).
  - [6] Xiaoxin Zhou and C.D. Lin, *Phys. Rev. A* **61**, 053411 (2000).
  - [7] E.Y. Sidky and C.D. Lin, *J. Phys. B* **31**, 2949 (1998).
  - [8] H.A. Kramers, *Collected Scientific Papers* (North-Holland, Amsterdam, 1956), p. 866.
  - [9] W.C. Henneberger, *Phys. Rev. Lett.* **21**, 838 (1956).
  - [10] R.M.A. Vivirito and P.L. Knight, *J. Phys. B* **28**, 4357 (1995).
  - [11] Q. Su, J.H. Eberly, and J. Javanainen, *Phys. Rev. Lett.* **64**, 862 (1990).
  - [12] K.C. Kulander, K.J. Schafer, and J.L. Krause, *Phys. Rev. Lett.* **66**, 2601 (1991).
  - [13] V.C. Reed, P.L. Knight, and K. Burnett, *Phys. Rev. Lett.* **67**, 1415 (1991).
  - [14] N.J. Kylstra, R.A. Worthington, A. Patel, P.L. Knight, J.R. Vázquez de Aldana, and L. Roso, *Phys. Rev. Lett.* **85**, 1835 (2000).
  - [15] J. Javanainen, J.H. Eberly, and Q. Su, *Phys. Rev. A* **38**, 3430 (1988).
  - [16] A.M. Popov, O.V. Tikhonova, and E.A. Volkova, *J. Phys. B* **32**, 3331 (1999).
  - [17] Q. Su, B.P. Irving, C.W. Johnson, and J.H. Eberly, *J. Phys. B* **29**, 5755 (1996).
  - [18] A. Patel, N.J. Kylstra, and P.L. Knight, *J. Phys. B* **32**, 5759 (1999).
  - [19] D. Barash, A.E. Orel, and R. Baer, *J. Phys. B* **33**, 1279 (2000).
  - [20] S. Geltman, *J. Phys. B* **32**, 853 (1999).
  - [21] Th. Mercouris and C.A. Nicolaides, *J. Phys. B* **32**, 2371 (1999).
  - [22] B. Sundaram and L. Armstrong Jr., *Phys. Rev. A* **38**, 152 (1988).

- [23] L.A. Collins and A.L. Merts, Phys. Rev. A **37**, 2415 (1988).
- [24] M. Gavrilă and J.Z. Kaminski, Phys. Rev. Lett. **52**, 613 (1984).
- [25] M. Pont and M. Gavrilă, Phys. Rev. Lett. **65**, 2362 (1990).
- [26] M. Dörr, R.M. Potvliege, D. Proulx, and R. Shakeshaft, Phys. Rev. A **43**, 3729 (1991).
- [27] L. Dimou and F.H.M. Faisal, Phys. Rev. A **49**, 4564 (1994).
- [28] U. Lambrecht, L. Dimou, and F.H.M. Faisal, Phys. Rev. A **57**, 2832 (1998).
- [29] R. Grobe and C.K. Law, Phys. Rev. A **44**, 4114 (1991).
- [30] J.H. Eberly, Phys. Rev. A **42**, 5750 (1990).
- [31] Q. Su and J.H. Eberly, Phys. Rev. A **44**, 5997 (1991).
- [32] M.P. de Boer, J.H. Hoogenraad, R.B. Vrijen, L.D. Noordam, and H.G. Muller, Phys. Rev. Lett. **71**, 3263 (1993).
- [33] Q. Su, Laser Phys. **3**, 241 (1993).